Inhaltsverzeichnis

Time behaviour and reflektivity of the self-pumped phase conjugation in fiber-like BTO crystals

M. Esselbach, G. Cedilnik, A. Kiessling, V. Prokofiev†, and R. Kowarschik

Self-pumped and mutually pumped phase conjugation based on the fanning effect is demonstrated in photorefractive BTO crystals with applied electric ac fields [1,2]. We used fiber-like crystals that enable a long interaction region and high applied electric fields.

We studied three types of phase conjugate mirrors (PCM). The first one is the self-pumped PCM (SPPCM, see figure 1) [3–6]. The holographic gratings are written by interference of signal wave and fanout [7]. A part of the fanout is reflected at the rear side of the crystal and acts as second pump wave for the four-wave mixing. The second type is the external SPPCM (ESPPCM, see figure 2) [8,9]. The arrangement is nearly the same as for the SPPCM, but the fanout is reflected at an external concave mirror. Higher reflectivity and faster response with respect to the SPPCM can be expected with this type [9]. The third type is the mutually pumped PCM (MPPCM). Mutually pumped phase conjugation is a principle where two incident signal waves experience phase conjugating reflection at the same time (see figure 3) [10]. The waves do not need to be mutually coherent.

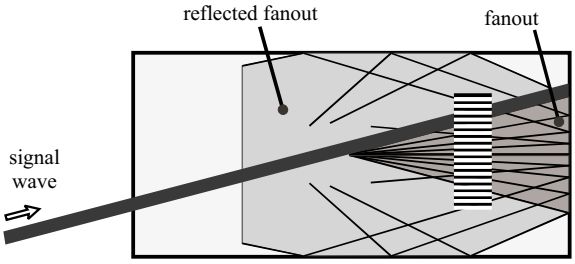

Fig. 1: SPPCM. The fanout is reflected at the rear side of the crystal.

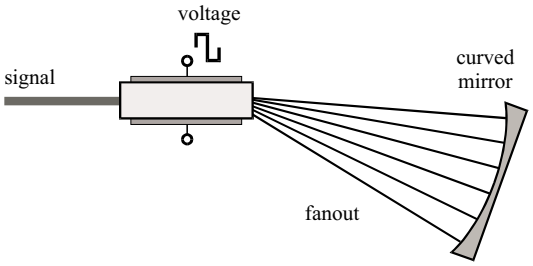

Fig. 2: ESPPCM. The fanout is reflected at an external curved mirror.

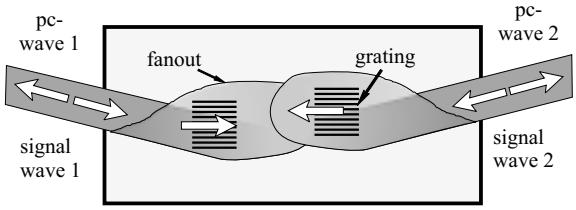

Fig. 3: MPPCM. Each reading pump wave needed for the phase conjugation of one signal wave is produced by the fanning of the other signal wave. Both signal waves will be phase conjugated at the same time.

Each signal wave interferes with its own fanout building a grating. Parts of these gratings are jointly used. Diffraction at these gratings leads to phase conjugation.

The arrangement shown in figure 4a is used to investigate the reflectivity and the temporal behaviour of the SPPCM and the ESPPCM. We used the unexpanded beam of a HeNe-laser

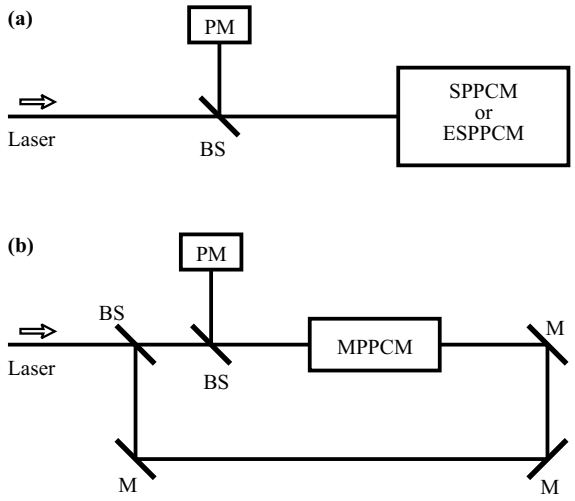

Fig. 4: Experimental arrangements. PM are power meters, BS are beam splitters, and M are mirrors.

($\lambda = 633\,\mathrm{nm}$) with a diameter of 1.6 mm. The light was polarised parallel to the [111] axis of the crystal and to the applied electric field. The external angle between the propagation direction of the signal wave and the normal of the front face of the crystal was 4°. Thus interaction between the input beam and its reflections from

†Väisälä Laboratory, Department of Physics, University of Joensuu, Finland

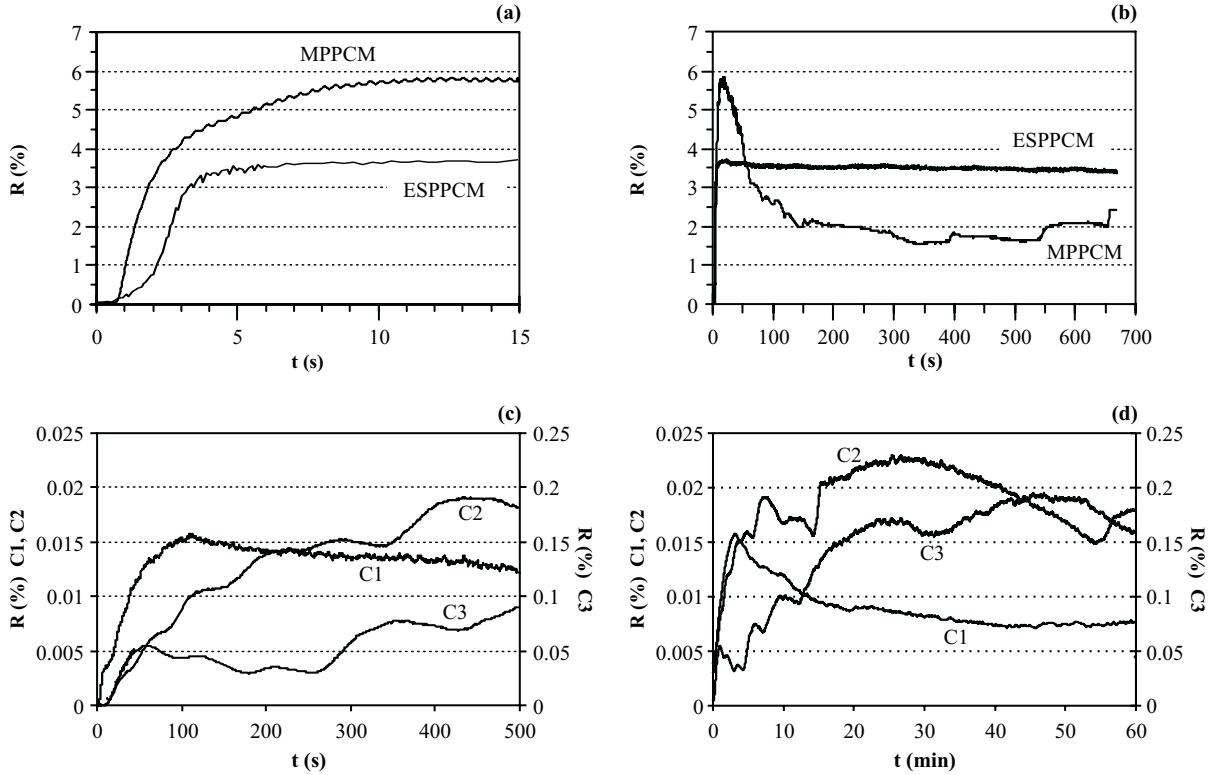

Fig. 5: Investigation of the temporal behaviour and the reflectivity. **(a)** Build-up of the phase conjugate reflection for ESPPCM and MPPCM. **(b)** Study of the long-time stability for ESPPCM and MPPCM. **(c)** and **(d)** Build-up and long-time stability of the phase conjugate reflection for the SPPCM. The conditions for the measurements are the same for all curves. Left axes of ordinates correspond to graphs C1 and C2 and the right axes to C3.

the rear side as well as direct reflections to the detector were mostly avoided. There were no additional reflections of the input beam at the inner sides of the crystal using this geometry. We used a concave mirror with a focal length of 75 mm in a distance of approxi-mately 150 mm to the centre of the crystal for the ESPPCM. This warrants a nearly perfect retro-reflection of the fanout into the region of its origin (see figure 2).

The arrangement of the MPPCM is shown in figure 4b. The principal geometry is the same as described above. The two waves incident to the crystal from opposite directions originate from one laser but are mutually incoherent in the crystal because of the different path lengths. They have the same intensity and polarisation angle.

The above mentioned types of PCM are tested with regard to temporal behaviour and reflectivity. The buildup behaviour and the stability of the reflectivity are of interest with respect to applications.

Results of measurements for the ESPPCM and the MPPCM are shown and compared in figures 5a and 5b (two different time scales). The measurements were done with relative low intensities of the incident waves of $0.8\,\mathrm{mW/mm^2}$ for the ESPPCM and $2 \cdot 0.8\,\mathrm{mW/mm^2}$ for the MPPCM.

The response time τ is defined as the time in which the reflectivity R reaches the value $(1 - 1/\mathrm{e}) \cdot R_{\max}$, where $R_{\max}$ is the maximum reflectivity. The response times τ were found to be 3.6 s for the ESPPCM and 2.3 s for the MPPCM. In reference [9] a response time of 150 s for the SPPCM and 8 s for the ESPPCM is reported for $BaTiO_3$ using an intensity of $0.3\,\mathrm{mW/mm^2}$. Reference [11] shows $\tau = 10\,\mathrm{s}$ for a SPPCM in $BaTiO_3$, [12] $\tau = 10 \ldots 20\,\mathrm{s}$ for SPPCM and ESPPCM, and [13] $\tau = 15\,\mathrm{s}$ for SBN (for $0.8\,\mathrm{mW/mm^2}$). Thereon it was shown that such PCM in BTO are comparable or even faster than known for barium titanate and SBN.

We note that the reversal of the applied electric field leads to momentary changes in the diffraction efficiency [14,15] that result in slight changes (fluctuations) in the reflectivity. These fluctuations were mostly filtered out in figure 5.

We realised reflectivities in the range of a few percent (approximately 4% for the ESPPCM and 6% for the MPPCM). With the MPPCM higher reflectivities for one wave can be reached by choosing a higher intensity of the second in-

cident wave. These values are far below the reflectivities of up to 60% found in $BaTiO_3$ [9,12].

Figure 5b shows the long time stability of both types of PCM. The reflectivity of the ESPPCM shows a high stability. The fluctuation are smaller than 3 % after the first 100 s. In contrast to the ESPPCM the reflectivity of the MPPCM strongly decreases (down to 25 % of the maximum value) and shows strong fluctuations as also known for barium titanate [16]. The higher stability of ESPPCM in $BaTiO_3$ was already demonstrated in [9,12].

Internally self-pumped phase conjugation was found to occur. Figure 5c shows the build-up of the phase conjugate reflection of the SPPCM. All the measurements (graphs C1, C2, C3) have been done under the same experimental conditions. The intensity of the incident signal wave was chosen to be $16\,\mathrm{mW/mm^2}$. This type of PCM did not run with an intensity as low as we used for the above mentioned types. The response times, which are in the range of minutes, are much longer than for ESPPCM and MPPCM in spite of the higher intensity. We measured $\tau_{C1} = 160\,s$, $\tau_{C2} = 390\,s$, and $\tau_{C3} = 330\,s$. The maximum reflectivities are $R_{C1} = 0.016\,\%$, $R_{C2} = 0.023\,\%$, and $R_{C3} = 0.2\,\%$ and are therefore much lower than for ESPPCM and MPPCM. The reason is that the reading pump wave is much weaker than the signal wave because of the low reflectivity at the back face and the geometrically unfavourable reflection (compared to the concave mirror in the ESPPCM). The strong variation of temporal response and reflectivity could be based on a very strong sensibility of the phase conjugate reflection on minimal deviation of the experimental conditions. Figure 5d shows measurements with respect to the long time stability. The strong temporal variations are obvious. These periodic or chaotic fluctuations are well known for self-pumped phase conjugate processes as self-organising processes [16,17]. The fluctuations of the reflectivity of the SPPCM are generally unsuitable for applications.

In conclusion, we have demonstrated the realizability of self-pumped (SPPCM), externally self-pumped (ESPPCM), and mutually pumped (MPPCM) phase conjugation in a fiber-like BTO crystal with applied electric ac field. Moderate intensities in the range of $1\,\mathrm{mW/mm^2}$ have been used. Reflectivities up to 6 % have been reached. Best results with respect to the stability were obtained with the ESPPCM. The advantage of using BTO is that the crystals are easier to grow, easier to produce with high optical quality, and cheaper compared with for instance $BaTiO_3$. Fiber-like crystals of BTO are promising candidates to realise self-pumped phase conjugation in applications.

References

[1] Esselbach M, Cedilnik G, Kiessling A, Baade T, Kowarschik R, J. Opt. A: Pure Appl. Opt. 1, 735 (1999)

[2] Esselbach M, Cedilnik G, Kiessling A, Kowarschik R, Prokofiev V, OSA TOPS 27, 314 (1999)

[3] Dou S X, et al., J. Opt. Soc. Am. B 12, 1048 (1995)

[4] Dou S X, et al., Appl. Opt. 34, 2024 (1995)

[5] Nowak A V, Moore T R, Fisher R A, J. Opt. Soc. Am. B 5, 1048 (1988)

[6] Eliseev V V, Zozulya A A, Bacher G D, and Feinberg J, J. Opt. Soc. Am. B 9, 1048 (1992)

[7] Rupp R A and Drees F W, Appl. Phys. B 39, 223 (1986)

[8] Esselbach M, Kiessling A, Rehn H, Fleck B, and Kowarschik R, J. Opt. Soc. Am. B 14, 846 (1997)

[9] Rehn H and Kowarschik R, Opt. Commun. 109, 155 (1994)

[10] Raita E, Kamshilin A A, Prokofiev V V, and Jaaskelainen T, Appl. Phys. Lett. 70, 1641 (1997)

[11] Suzuki T and Sato T, Appl. Opt. 32, 3959 (1993)

[12] Krause A, Notni G, Wenke L, Opt. Mat. 4, 386 (1995)

[13] Miller M J, Sharp E J, Wood G L, Clark III W W, Salamo G J, Neurgaonkar R R, Opt. Lett. 12, 340 (1987)

[14] Shamonina E, Ringhofer K H, Sturman B I, Kamenov V P, Cedilnik G, Esselbach M, Kiessling A, Kowarschik R, Kamshilin A A, Prokofiev V V, Jaaskelainen T, Opt. Lett. 23, 1435 (1998)

[15] Esselbach M, Cedilnik G, Kiessling A, Kowarschik R, Kamshilin A A, Prokofiev V V, and Jaaskelainen T, OSA TOPS 27, 383 (1999)

[16] Rauch T, Denz C, Tschudi T, Opt. Commun. 88, 160 (1992)

[17] Jeffrey P M and Eason R W, J. Opt. Soc. Am. B 11, 476 (1994)

Transfer or imaging of intensity and phase distributions with fiberlike BTO crystals

M. Esselbach, G. Cedilnik, A. Kiessling, V. Prokofiev†, and R. Kowarschik

External self-pumped and mutually pumped phase conjugate mirrors (ESPPCM and MPPCM) in fiber-like BTO crystals with applied electric ac fields are studied. Experimental results characterising the the reflection of intensity and phase patterns, and the quality of the phase conjugation are presented [1,2].

The arrangement shown in figure 1 is used to investigate the imaging properties of the ESPPCM. The laser beam is expanded to a diameter of approximately 20 mm. This expanded

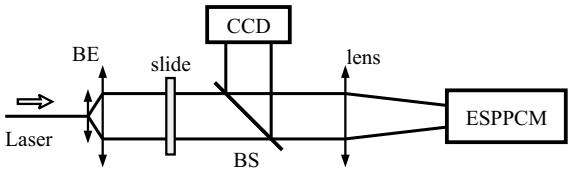

Fig. 1: Arrangement to study the imaging quality of the ESPPCM. BS is a beam splitter and BE a beam expander.

beam is focused by a lens with a focal length of 200 mm to the BTO crystal in such a way that the focal point is 5 mm behind the crystal. A slide is placed within the expanded beam. The camera is placed in the same distance from the beam splitter as the slide to ensure real imaging. A symmetrical square wave voltage of 5.0 kV and 50 Hz was applied to the crystal in all arrangements leading to an applied field of 1.5 kV/mm.

We studied how an intensity structure is reflected or imaged by an ESPPCM. The results are shown in figure 2. Picture (a) shows the intensity distribution of the phase conjugated wave if a expanded signal wave with spatial homogenous intensity is used. The speckle-like structure is a common property of such PCM based on fanning. We introduced a slide with the picture shown in figure 2b (size approximately 2×2 cm) that acts as an amplitude object in the signal wave. The result of lensless imaging by phase conjugation is shown in (c). This phase conjugated reflection is compared with the reflection (no imaging) at a conventional plane mirror (d). The quality of the resulting picture

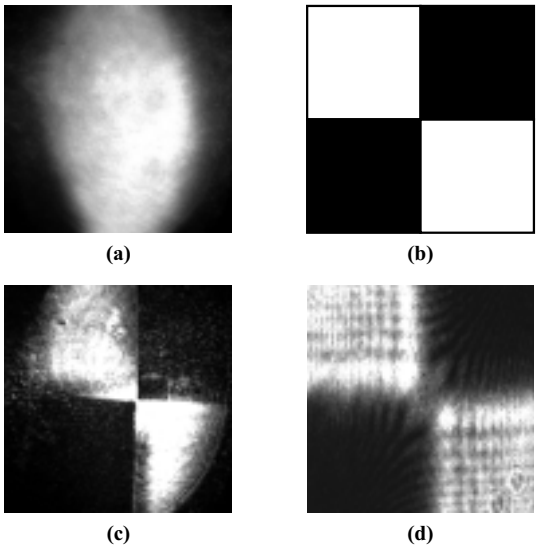

Fig. 2: Imaging of intensity structures by an ESPPCM. **(a)** Intensity distribution of the pc-wave, **(b)** slide, **(c)** intensity structure imaged by pc-reflexion, and **(d)** intensity structure reflected by a conventional plane mirror.

(d) is lower because of diffraction as can be seen at the edges (high spatial frequencies).

The imaging properties of the MPPCM were investigated using an unexpanded laser beam as signal wave. Figure 3 shows the intensity distribution of the reflected wave projected onto a screen. A disadvantage of this method soon

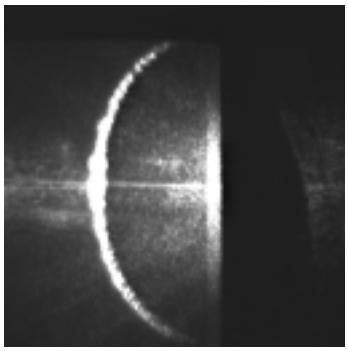

Fig. 3: Intensity structure of the phase conjugated wave in case of an unexpanded signal beam using a MPPCM.

becomes obvious. The intensity of the reflected signal forms a part of a ring structure. The reason is the structure of the fanout in space [3], it forms a cone. Therefore, there are additional gratings that are not built by the interference

†Väisälä Laboratory, Department of Physics, University of Joensuu, Finland

of signal and fanout, but by the interference of different parts of the fanout. This system of gratings is read out by the fanout of the other wave which is also cone shaped. This results in an output signal that consists of waves that lie on the surface of a cone and therefore build the intensity distribution shown in figure 3. Mutually pumped phase conjugation was shown for $BaTiO_3$ too. The coupling in this medium is very anisotropic because of the very different coefficients of the electrooptic tensor. The additional gratings are suppressed by a self-organising process. After a certain time only gratings yielding phase conjugation exist. In BTO this is not the case. This distortion can only be partially avoided if the signal wave is not plane but has a phase structure, what could limit the applicability. Such rings have not been observed with the ESPPCM.

We evaluated the quality of phase conjugation [4], i.e. how accurately the phase distribution of a wave is reflected by a PCM. Because of the better stability and reflection of intensity structures we concentrate on the ESPPCM.

A special feature of the phase conjugation is the so called aberration compensation [5,6], that is often used in devices with PCM [5,7]. If a signal wave with plane wave front passes a phase object introducing a phase distortion then is reflected at a PCM and passes the same distortion once more in opposite direction the distortion is repaired [8] and the wave is plane again [6].

Figure 4a shows a modified Michelson interferometer where one mirror is a PCM. Because of

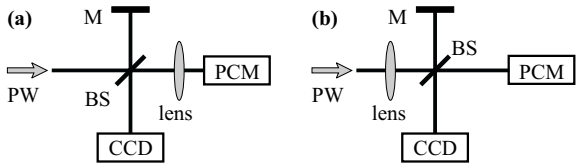

Fig. 4: Michelson interferometer with PCM. (a) Using the aberration compensation. (b) Entrance interferometer. PW is a plane wave, BS are beam splitters, and m are mirrors.

the above mentioned feature the phase distortion introduced by a lens into the interferometer arm with PCM should be corrected. We sent a plane wave to the interferometer and got parallel fringes (see figure 5a) as the interference pattern of two plane waves at the exit of the interferometer. This means that the phase distortion was corrected and therefore the phase conjugation works fine.

The spatial phase distribution of a phase conjugated wave was measured and compared with the phase distribution of the original wave in order to study the quality of the phase conjugation quantitatively.

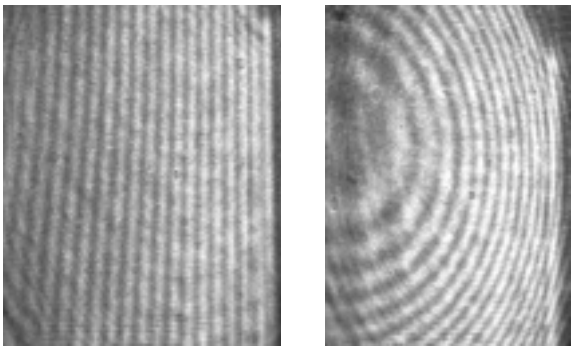

Fig. 5: Measurements with the Michelson interferometer with PCM. (a) Interferogram of a plane wave demonstrating the aberration compensation using a PCM. (b) Interferogram of a spherical wave demonstrating the possibilities of an entrance interferometer.

For that purpose we used the so-called SWIM interferometer (signal wave intensity measuring interferometer [9]) that is shown in figure 6. It

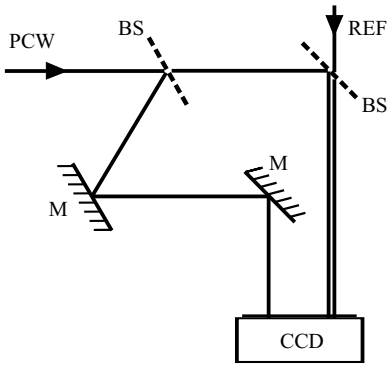

Fig. 6: SWIM interferometer. PCW is the phase conjugated wave and REF is the plane reference wave.

enables the simultaneous recording of interference pattern and intensity distribution of the wave under consideration on separate areas of a CCD camera within one shot. This is an advantage if the intensity of the wave to be measured is not homogeneous what is the case for the waves that are phase conjugated using the PCM presented in this paper (see figure 2a). Using other interferometers one has to determine the unknown intensity distribution with a second measurement or to use Fourier filtering with its limitations. The device is a compact module that can directly be mounted on a standard CCD camera.

The spatial phase distribution of the pha-

se conjugated wave of a plane signal wave was measured. Figure 7a shows the phase along one arbitrary line within the two-dimensional measured phase distribution. Comparison of this

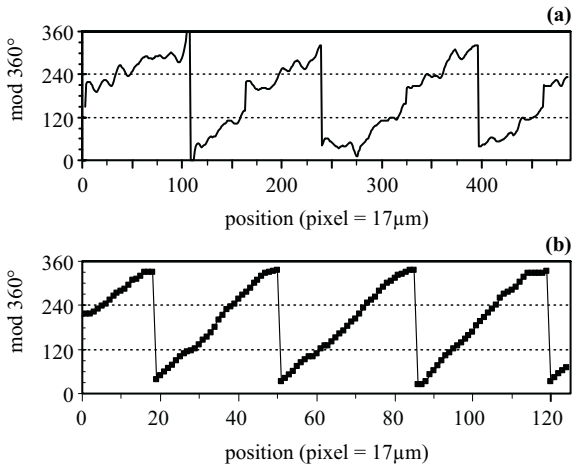

Fig. 7: Phase scan of the phase conjugated wave (a) and a plane wave (b). Steps at $\Delta\phi = n \cdot 180°$ are due to the singularities of the arccos-function. The phase-speckles are about $2\pi/15$.

result to the result of the direct measurement of the plane signal wave (figure 7b) demonstrates that the phase conjugated wave is plane too. The quality of the phase conjugation is determined by a phase noise in the range of $2\pi/15$ that is added to the signal wave by the process of phase conjugation.

Another feature of an interferometer with PCM is that one can directly measure the phase distribution of an input wave with double sensitivity (entrance interferometer [8,11]). The arrangement shown in figure 4b is used to demonstrate the applicability of the ESPPCM for this purpose.

We used this interferometer in order to measure the spherical wave that was produced by introducing a lens into the path of the plane signal wave. Figure 5b shows the interferogram recorded by the CCD camera. The concentric circles, which are not seen with a conventional interferometer, demonstrate that this interferometer and therefore the ESPPCM works.

We have demonstrated the transfer of intensity and phase patterns by ESPPCM and MPPCM in fiber-like BTO crystals with applied electric ac field. The ESPPCM shows the best imaging properties for intensity structures. The quality of phase conjugation was tested. A phase noise of only $2\pi/15$ was measured for the phase conjugate reflection with the ESPPCM. Fiber-like crystals of BTO are promising candidates to realise self-pumped phase conjugation in applications.

References

[1] Esselbach M, Cedilnik G, Kiessling A, Baade T, Kowarschik R, J. Opt. A: Pure Appl. Opt. 1, 735 (1999)

[2] Esselbach M, Cedilnik G, Kiessling A, Kowarschik R, Prokofiev V, OSA TOPS 27, 314 (1999)

[3] Byron Q, Yeh P, Gu C, and Neurgaonkar R R, J. Opt. Soc. Am. B 9, 114 (1992)

[4] Xie P, Dai J-H, Wang P-Y, and Zhang H-J, Opt. Commun. 130, 302 (1996)

[5] Kiessling A, Baade T, and Wenke L, J. Mod. Opt. 43, 1525 (1996)

[6] Yariv A, IEEE Journal of Quantum Electronics QE-14, 650 (1978)

[7] Chen W H, Wang P J, San P C, and Yeh P, SPIE Vol. 739, 105 (1987)

[8] Gauthier D J, Boyd R W, Jungquist R K, Lisson J B, and Voci L L, Opt. Lett. 14, 323 (1989)

[9] Cedilnik G, Kiessling A, Kowarschik R, Proc. LASERS'98, Tucson (AZ) USA, 1110 (1999)

[10] Howes W L, Appl. Opt. 25, 3167 (1986)

Applying electric fields to Sillenite crystals for two-wave mixing

M. Esselbach and G. Cedilnik

Using the band transport model and the KUKHTAREV equations it is possible to calculate the space charge field E_{sc} that builds up in a photorefractive medium. In order to allow to find an analytic solution for the steady state a number of limiting assumptions and the validity of approximations are necessary. That are in detail:

- small modulation depth of the writing intensity structure ($m \ll 1$)
- a charge transport length that is small compared to the grating period ($l_{CT} \ll \Lambda$)
- only one type of charge carriers
- only one donor and one acceptor level
- neglectable thermal excitation
- proportionality between rate of excitation and intensity
- occupied acceptor density much smaller then donor density $N_{\mathrm{A}}^{-} \ll N_{\mathrm{D}}$
- small number of exited donors compared to their total number ($N_{\mathrm{D}}^{+} \ll N_{\mathrm{D}}$), i.e. small number of free charge carriers
- harmonic shape of the intensity distribution and of all distributions following from it (e.g. ρ_{sc} and E_{sc}) [1,2]

The solution for the stationary amplitude of the modulated space charge field E_1 is [1–3]

$$E_1 = m \frac{i\,E_{\mathrm{d}}}{1+\frac{E_{\mathrm{d}}}{E_{\mathrm{q}}}} \left[\frac{1+i\left(\frac{E_0}{E_{\mathrm{d}}}\right)}{1+i\left(\frac{E_0}{E_{\mathrm{d}}+E_{\mathrm{q}}}\right)} \right], \qquad (1)$$

with $E_{\mathrm{d}} = \frac{K\,k_B\,T}{q}$ and $E_{\mathrm{q}} = \frac{q\,N_{\mathrm{A}}}{K\varepsilon}$, where q is the unit charge, K the absolute value of the grating vector, and ε the dielectric constant. E_{d} is the so-called diffusion field. E_{q} is the saturation field, i.e. it is the maximum field for a given acceptor density N_{A}. E_0 is an electric field that is externally applied to the photorefractive crystal.

The term ahead of the bracket on the right side of equation (1) is the amplitude of the space charge field that builds up in case no external field is applied ($E_0 = 0$). The term in brackets represents a scaling factor which describes the influence of an external electric field. The absolute value of this factor in dependence on the strength of the external field is shown in fig. 1

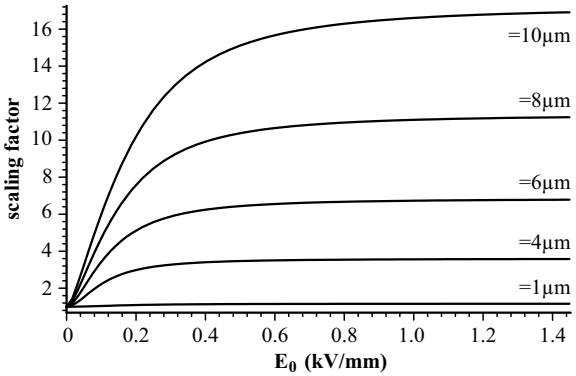

Fig. 1: Absolute value of the scaling factor according to eq. (1) as a function of the applied DC field E_0 for various values of the grating period. $T = 293\,\mathrm{K}$, $N_{\mathrm{A}} = 0.5 \cdot 10^{21}\,\mathrm{m}^{-3}$, $\varepsilon_{\mathrm{rel}} = 56$.

for certain values of the grating period Λ. A set of material parameters for a typical BSO crystal is used.

It is possible to increase the amplitude of the modulated space charge field by applying an external electric DC field and with that to increase the interaction of the interfering waves. On the other hand such a DC field leads to a transition from the pure diffusion to the drift case, what means that drift in the electric field is the dominating charge transport process. The deviation of the phase shift ϕ between the gratings of intensity and refractive index from the value $\pi/2$,that is caused therefore, results in a decrease of the energy coupling between the waves.

This can be avoided by using AC fields with a period that is much shorter than the photorefractive response time. In this case there is no preferred direction of charge carrier movement and that way one has in principal the same situation as with diffusion only. Especially fields of square wave form are suited as shown in [4]. The space charge field is then given by [5]

$$\Im(E_1) = |E_1| = m \frac{E_0^2\,E_{\mathrm{q}}}{E_0^2 + E_{\mathrm{M}} E_{\mathrm{q}}}, \qquad (2)$$

where $E_{\mathrm{M}} = (K\mu\tau_{\mathrm{e}})^{-1}$ (τ_{e} lifetime of a charge carrier in the conduction band, μ mobility). Neglecting absorption, the gain G is

$$G = \frac{1+m_{\mathrm{v}}}{1+m_{\mathrm{v}}\,\mathrm{e}^{-\frac{\pi\,n_0^3\,r_{\mathrm{eff}}}{\lambda\cos(\theta/2)}\,|E_1|\,L}}, \qquad (3)$$

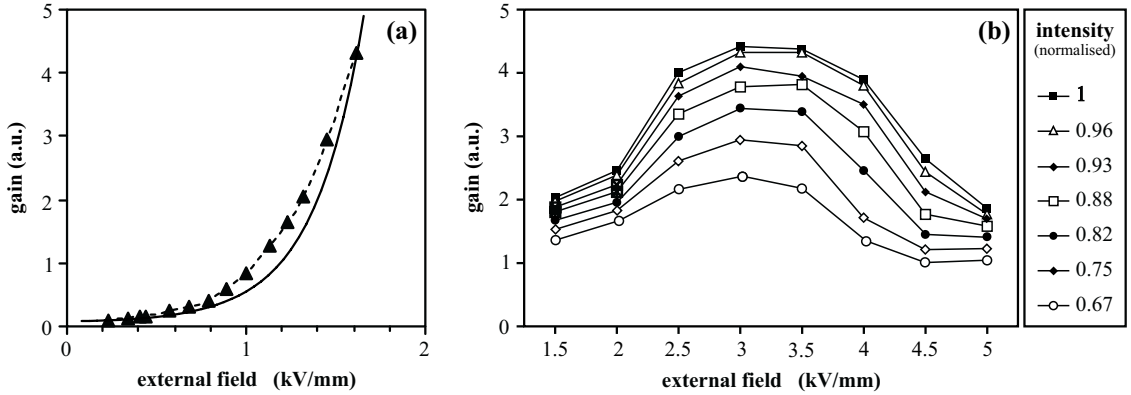

Fig. 3: Measurement of the TWM gain as a function of E_0. **(a)** crystal width 4.4 mm, $I_0 = 14\,\mathrm{mW/mm^2}$, $m_\mathrm{v} = 267$. Solid line according to eq. (3). **(b)** crystal width 1 mm, $I_0 = 14\,\mathrm{mW/mm^2}$, $m_\mathrm{v} = 14$.

where m_v is the intensity ratio of the two waves and L is the interaction length. The course of the function $G = f(E_0)$ is shown in fig. 2. There

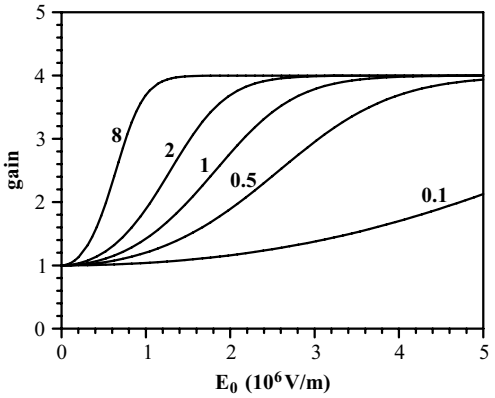

Fig. 2: Calculated gain as a function of the applied AC field E_0 for various values of $\mu\tau_\mathrm{e}$ (in $10^{-12}\,\mathrm{m^2/V}$). $T = 293\,\mathrm{K}$, $N_\mathrm{A} = 7 \cdot 10^{22}\,\mathrm{m^{-3}}$, $\varepsilon_\mathrm{rel} = 47$, $m_\mathrm{v} = 3$, $r_\mathrm{eff} = 5.17 \cdot 10^{-12}\,\mathrm{m/V}$, and $\theta = 4°$.

is an increase and a saturation for higher fields.

Fig. 3 shows results of measurements of the dependence $G = f(E_0)$ for applied electric AC fields for two different BTO samples. Very strong fields are only possible for the more narrow one in fig. 3b. The results in fig. 3a meet the expectations, e.g. an increase of the interaction efficiency with increasing electric field. A curve according to eq. (3) fits well to the experimetal data (solid line in the figure).

The maxima in fig. 3b appear for fields between 3 kV/mm and 3.5 kV/mm [6]. The initial increase in direction of stronger electric fields can be explained as said but not the decrease after passing the maximum, at least only in attempt [7].

A possible explanation is given by the band transport model of Kukhtarev. One of the above mentioned conditions is that the charge transport length is assumed to be small with respect to the grating period ($l_\mathrm{CT} \ll \Lambda$). This ensures that the excited electrones recombine preferably in dark regions. Under the influence of an external field, the charge carriers cover on average a distance of $l_\mathrm{D} = \mu\tau_\mathrm{e}E_0$. If that condition is not longer fulfilled with strong fields E_0, the probability of a recombination in bright regions increases [8]. This yields a decrease of the modulation of the charge density and of the space charge field and therefore a decrease of the gain.

Another aspect is that the condition $T_\mathrm{HV} \ll \tau_\mathrm{g}$ (T_HV period of the voltage supply, τ_g grating buildup time) can be not well fulfilled for a finite frequency of the AC field. This would lead to $\phi \neq \pi/2$ and therefore to a decrease of the gain [8].

Applying electric fields for TWM in Sillenites enables the interaction of the waves to be intensified.

References

[1] Yeh P, Wiley Series in Pure and Applied Optics, John Wiley & Sons, New York (1993)

[2] Solymar L, Webb D J, Grunnet-Jepsen G, Progress in Quantum Electronics 18, 377 (1994)

[3] Kukhtarev N V, Markov V B, Odulov S G, Soskin M S, Vinetskii V L, Ferroelectrics 22, 949 (1979)

[4] Stepanov S I, Petrov M P, Opt. Comm. 53, 292 (1985)

[5] Solymar L, Webb D J, Grunnet-Jepsen G, Oxford Series in Optical and Imaging Sciences, Clarendon (1996)

[6] Esselbach M, Cedilnik G, J. Mod. Optics, accepted for publication (1999)

[7] Khomenko A V, Garcia-Weidner A, Kamshilin A A, Opt. Lett. 21, 1014 (1996)

[8] Kawata Y, Kawata S, Optik 90, 27 (1992)

Determination of material parameters with TWM in photorefractive crystals

M. Esselbach, G. Cedilnik, A. Kiessling, E. Nippolainen†, and R. Kowarschik

Studies of the two-wave mixing in photorefractive crystals, here especially Sillenites, enable to determine certain material parameters and to get information about their band structure and occupancy.

The influence of the period Λ of the index grating on the gain G is investigated. The amplitude of the space charge field E_1 that builds up within the crystal by the interaction of two waves is a function of three characteristic quantities which have the dimension of an electric field and that are called diffusion field (E_d), saturation field (E_q), and drift field (E_μ). They are defined by

$$E_\mathrm{d} = \frac{K\,k_\mathrm{B}\,T}{q}\,,\; E_\mathrm{q} = \frac{q\,N_\mathrm{A}}{K\varepsilon}\,,\; E_\mu = (K\mu\tau_\mathrm{e})^{-1}\,,$$

where k_B is the BOLTZMANN constant, T the temperature, q the unit charge, N_A the acceptor density, ε the dielectric constant, τ_e the lifetime of a charge carrier in the conduction band, and μ the mobility. They are functions of the absolute value of the grating vector $K = |\vec{K}|$ and thus functions of the grating period Λ. Neglecting absorption, the gain $G(K)$ is given by

$$G(K) = \frac{1+m_\mathrm{v}}{1+m_\mathrm{v}\,\mathrm{e}^{-\frac{\pi\,n_0^3\,r_\mathrm{eff}}{\lambda\cos(\theta/2)}\,|E_1(K)|\,L}}\,,$$

where m_v is the intensity ratio of the two waves and L is the interaction length within the crystal. This function has a maximum at a position that depends on the acceptor density N_A. Therefore, it is possible to determine N_A by measuring the angle ϑ between the interacting beams, where maximal gain appears.

We used fiberlike BTO and BSO crystals for our experiments, where it is possible to apply strong electric AC fields. An effect called *giant momentary readout* [1–4] that appears using this crystals and yields short gain peaks makes it necessary to decide between mean and peak gain and to measure them for a series of angles.

Results of measurement are shown in fig. 1. The gain maximum appears at $\Lambda = 6.7\,\mu$m ($\widehat{=}\,150\,$lines/mm $\widehat{=}\,\vartheta = 5.4°$) for the peaks and at $\Lambda = 7.8\,\mu$m ($\widehat{=}\,128\,$lines/mm) for the mean gain level. For BSO we found the maximum at $\Lambda = 9.1\,\mu$m [5].

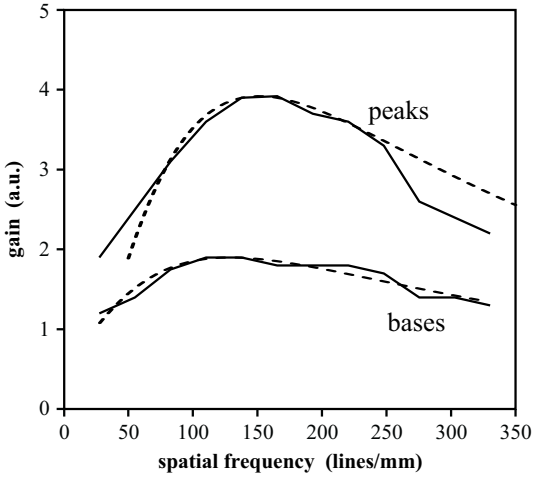

Fig. 1: TWM gain as a function of the grating period. Dashed lines represent functions that are fitted according to $G = G(\Lambda)$). $I_\mathrm{s} = 1\,\mathrm{mW/mm^2}$, $I_\mathrm{p} = 14\,\mathrm{mW/mm^2}$, $U_0 = 2\,\mathrm{kV}$, BTO $1.85 \times 3.84 \times 8.1\,$mm.

It is possible to fit functions according to $G = f(\Lambda, N_\mathrm{A})$ to the measured curves (see solid lines in fig. 1) using N_A as a variable parameter and that way to determine it. We get $N_\mathrm{A} = 5\ldots7\cdot 10^{22}\,\mathrm{m^{-3}}$, what is in the range that is given in the literatur [6,7]. For BSO we measured $N_\mathrm{A} = 4\cdot10^{22}\,\mathrm{m^{-3}}$.

All these measurements require the scanning of a range of angles in order to find the maximum TWM efficiency. Another method that uses the fanning effect makes this unnecessary. Fanning appears with these fiberlike Sillenite crystals because high gain can be reached applying strong AC fields. By this multi-two-wave mixing process the initially in all directions propagating scattered light is asymmetrically amplified by the signal wave according to the dependence $G = G(\Lambda)$. Because the scattering at crystal inhomogeneities provides a large angle spectrum one can record the curve of amplification as a function of Λ within one measurement by a line scan of a CCD camera picture.

Fig. 2 shows the experimental arrangement used to study the intensity distribution of the fanout and with this the gain distribution along

†Väisälä Laboratory, Department of Physics, University of Joensuu, Finland

the x-axis. With this setup no mechanical mo-

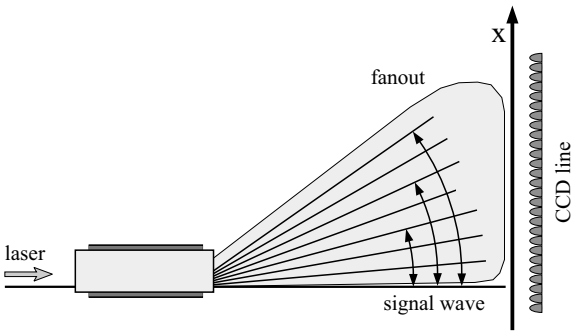

Fig. 2: Experimental arrangement for the measurement of $G = f(x) = f(\Lambda)$.

ving and adjusting as for normal TWM angle scanning is necessary.

Fig. 3 shows the intensity distribution of the fanout along the x-axis. Quasi steady state means that we worked with a higher frequency f_{HV} of the voltage supply, where the short gain peaks mentioned before are not of importance. There is a maximum of the gain, e.g. a

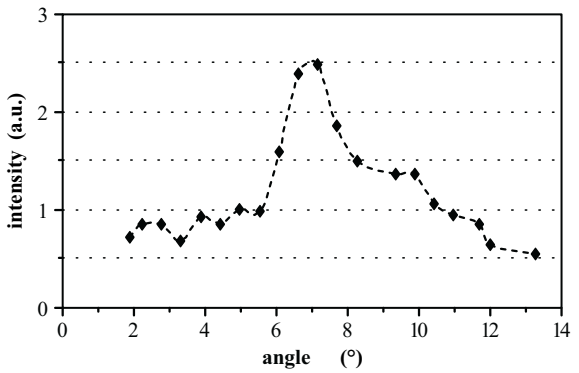

Fig. 3: Intensity distribution of the fanout for an angle range in the quasi steady state. $I_0 = 10\,\mathrm{mW/mm^2}$, $f_{\mathrm{HV}} = 200\,\mathrm{Hz}$, $E_0 = 2.8\,\mathrm{kV/mm}$, BTO $1 \times 7 \times 20\,\mathrm{mm}$. The dashed line is a guide to the eye.

concentration of the fanout [8], at $\vartheta \approx 7°$, what deviates from the value $\vartheta = 5.4°$ that was determined by simple TWM. An explaination is given by the fact that there is not only an energy transfer from the signal wave to a certain fanout wave but from all other fanout waves to this wave too. One would have to integrate over an angle range what would yield to a real optimum angle ϑ of less then 7°. For an application of this method this would have to be exactly studied and calculated.

In principle the described methods are suited to determine the number density N_{A}.

Acknowledgement

We would like to thank V. Prokofiev of the university of Joensuu (Finland) for the preparation of the fiberlike BTO and BSO crystals.

References

[1] Esselbach M, Cedilnik G, J. Mod. Optics, accepted for publication (1999)

[2] Esselbach M, Cedilnik G, Kiessling A, Kowarschik R, Proc. LASERS'98, Tucson (AZ) USA, 1138 (1999)

[3] Esselbach M, Cedilnik G, Kiessling A, Kowarschik R, Kamshilin A A, Prokofiev V V, Jaaskelainen T, OSA TOPS 27, 383 (1999)

[4] Esselbach M, Cedilnik G, Kiessling A, Kowarschik R, SPIE 3749, 268 (1999)

[5] Cedilnik G, Esselbach M, Kiessling A, Kowarschik R, Kamshilin A A, Shamonina E, Ringhofer K-H, J. Appl. Phys. 85, 1317 (1999)

[6] Millerd J E, Garmire E M, Klein M B, Wechsler B A, Strohkendl F P, Brost G A, J. Opt. Soc. Am. B 9, 1449 (1992)

[7] Raita E, Kamshilin A A, Jaaskelainen T, J. Opt. Soc. Am. B 7, 2023 (1998)

[8] Nippolainen E, Prokofiev V V, Kamshilin A A, Jaaskelainen T, Cedilnik G, Esselbach M, Kiessling A, Kowarschik R, OSA TOPS 27, 333 (1999)

Barium-Calcium-Titanate — A high gain photorefractive medium

M. Esselbach, E. Weidner, A. Kiessling, G. Cedilnik, and R. Kowarschik

Barium-Calcium-Titanat (BCT) is a relatively new and until now little investigated ferroelectric photorefractive storage medium.

The crystal has tetragonal structure at room temperature and is optically uniaxial. The manufacturing of BCT is easier than of Bariumtitanate (BT) [1]. The nominally undoped crystals with the formula $Ba_{0,77}Ca_{0,23}TiO_3$ are grown from a congruently melting composition of Bariumtitanate und Calciumtitanate [2,3], where the possible speed of crystal pulling is many times (about 15×) over that for BT. The BCT crystals can be considerable bigger [4] what is especially interesting for the application in the optical data storage. We used a crystal with dimensions $1 \times 1 \times 1\,\mathrm{cm}$ for our measurements.

The *single domain* structur is reached by poling in an external electric DC field near the phase transition temperatur of 98 °C [2]. Besides many common properties [5], unlike BT there is no further phase transition at a lower temperatur near 0 °C [1] that would change the crystal structure and therefore make the medium unsuited for optical data storage [6]. The usable electrooptic coefficients are partially larger than for BT [6,7]. Because of all these properties BCT seems to be a promising candidate for optical information storage [8].

Unlike BT there is considerable two-wave mixing (TWM) also for ordinary polarised light, what is because of the values of the components of the electrooptic Tensor [8]. Fig. 1 shows the temporal course of the amplification V of the signal wave I_s for ordinary and extraordinary polarised light. V is defined by $V = I_\mathrm{s}\mathrm{out}/I_\mathrm{s}\mathrm{in}$, where $I_\mathrm{s}\mathrm{in}$ and $I_\mathrm{s}\mathrm{out}$ are the intensities of the signal wave before and after passing the crystal with the pump wave on.

The response for extraordinary polarisation is remarkably slower than for ordinary polarisation. The reason is the initial energy loss of the pump wave to the advantage of the fanning.

The response times are with 5 s and 10 s in the same range as in reference [4] determined for an iron doped crystal. Therefore one can conclude that such a doping does not strongly influence the response times.

Fig. 2 shows the amplification of the signal

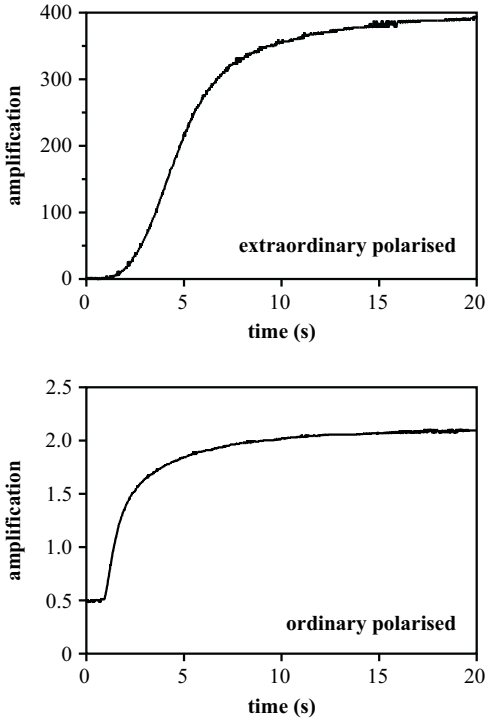

Fig. 1: Temporal course of the amplification by TWM in BCT for extraordinary and ordinary polarised light. $I_\mathrm{s} = 1\,\mu\mathrm{W/mm^2}$ and $I_\mathrm{p} = 10\,\mathrm{mW/mm^2}$, angle ϑ between signal and pump wave 45°.

wave in dependence on the intensity ratio m_v of pump and signal wave. Two series are measured in order to demonstrate the reproducibility of the measurement.

It appears that especially in the small signal range ($m_\mathrm{v} \gg 1$) high amplifications are reached (up to $V = 68000$). This dependence can be well described by [9]

$$G = \frac{I_\mathrm{s}(L)}{I_\mathrm{s}(0)} = \frac{1 + m_\mathrm{v}}{1 + m_\mathrm{v}\,\mathrm{e}^{-\gamma L}}\,\mathrm{e}^{-\upsilon L}\,, \qquad (1)$$

where L is the length of the interaction area, and υ is the absorption constant. Curves according to this equation are shown in fig. 2 and fit well to the measured values. The exponential gain factor γ (also called coupling constant) could be determined to $\gamma = 50 \ldots 55\ \mathrm{cm^{-1}}$. The energy coupling in BCT is far stronger as in BT [10]. Therefore, BCT turns out to be a high efficient medium for optical signal amplification [8].

High values of m_v ($m_\mathrm{v} \gg 1$) mean a small visibility m of the intensity distribution within

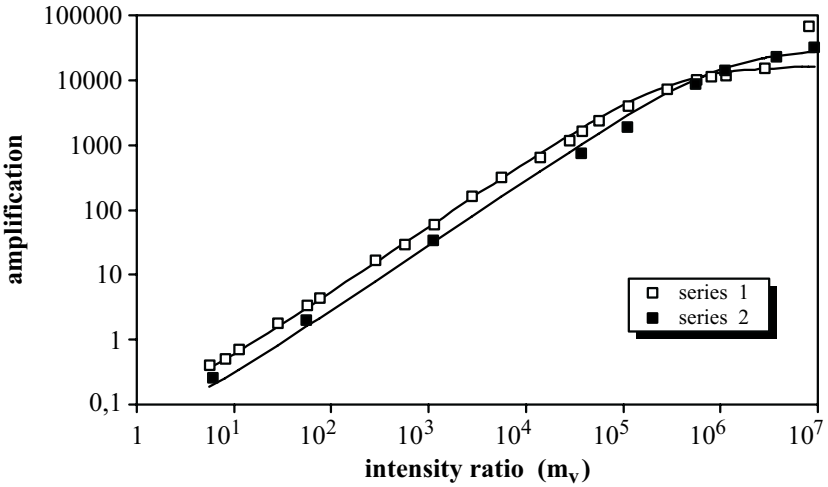

Fig. 2: Signal amplification in dependence on the intensity ratio m_v of pump and signal wave. The solid lines are calculated according to equation (1).

the medium and therefore (because of their proportionality) a small refractive index modulation n_1. Because of the strong coupling, the visibility m within the interaction region for large m_v is increased to values that enable a considerable modulation of the refractive index that is usable for information processing. In experiments the writing of hologramms could be demonstrated for intensity ratios as high as $m_\mathrm{v} = 10^8$ and $m = 10^{-4}$. A limitation was given only by the available detector. Because of this, it is necessary to pay increased attention to coherent scattered light which is often unavoidable in an experimental arrangement.

Barium-Calcium-Titanate is a promising candidate for optical information processing and information storage.

References

[1] Buse K, Appl. Phys. B 64, 391 (1997)

[2] Kuper Ch, Pankrath R, Hesse H, Appl. Phys. A 65, 301 (1997)

[3] Simon M, Mersch F, Kuper C, Mendricks S, Wevering S, Imbrock J, Krtzig E, Phys. Stat. Sol. (a) 159, 559 (1997)

[4] Korneev N, Mayorga D, Stepanov S, Veenhuis H, Buse K, Kuper C, Hesse H, Krtzig E, Opt. Comm. 160, 98 (1999)

[5] Schirmer O F, Mazur A, Veber C, Rdiger A, OSA TOPS 27, 149 (1999)

[6] Bernhardt S, Delaye P, Hesse H, Rytz D, Roosen G, OSA TOPS 27, 132 (1999)

[7] Kuper Ch, Buse K, van Stevendaal U, Weber M, Leidlo T, Hesse H, Krtzig E, Ferroelectrics 208, 213 (1998)

[8] Esselbach M, Kiessling A, Kowarschik R, SPIE 3749, 450 (1999)

[9] Yeh P, Wiley Series in Pure and Applied Optics, John Wiley & Sons, New York (1993)

[10] Colin J, Bann S, Rajbenbach H, Huignard J-P, Appl. Opt. 36, 9304 (1997)

Self-enhanced diffraction in Barium-Calcium-Titanate

M. Esselbach, A. Kiessling, G. Cedilnik, and R. Kowarschik

If a hologram is written into a photorefractive medium and read out in the following by the pump wave alone, it will be erased. In a medium such as BCT in which high amplification can be realised with TWM, an effect can appear that is called *self-enhanced diffraction* (SED, [1]).

Figure 1 shows the principle. The pump wave is diffracted at the refractive index grating that was created by the interference of signal and pump wave within the interaction region before. The result is a pair of waves, the reconstructed signal wave $\mathbf{S}'$ and the transmitted part of the pump wave $\mathbf{P}'$ (fig. 1a). These waves interfere and create a grating that is an exact phase correct copy of the original one. The hologram is rebuilt that way (fig. 1b) although the read out causes an erasing of the grating.

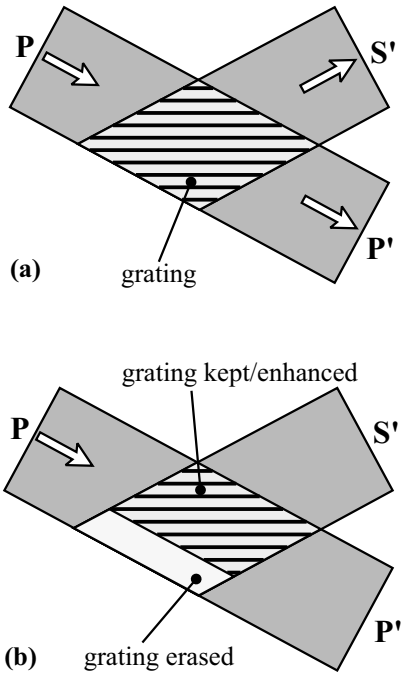

Fig. 1: Self-enhanced diffraction (schematic). **(a)** Creation of two waves by diffarction. **(b)** Unavoidable erasure.

In dependence on the initial modulation n_1 of the grating in can be kept, what means that it is stable against erasure during read out, or there can even be an enhancement of the grating modulation.

This effect can be used in order to refresh badly preserved or even partially erased holograms [1]. Within a periodically recurring process the hologram is alternating read from both sides what causes a gradual enhancement of the modulation depth n_1. Using Barium-Calcium-Titanate (BCT) this technique can be applied with cw-lasers instead of pulsed laser as in [1] because low intensities are sufficient.

The hologram can not be kept for any length of time. Fig. 1b shows why. The grating is only rewritten at locations where $\mathbf{S}'$ exists. Because this wave is created by diffraction of $\mathbf{P}$, a progressive erasure of the grating appears from the propagation direction of the initially incident signal wave. Therefore, SED can reach the enhancement of n_1 only at the expense of the thickness of the grating. An optimum with respect to the diffraction efficiency can be found.

The SED can be applied advantageously if the information that is to store in form of a hologram is available only for a short time periode [2] that is not long enough to reach the saturation level of the refractive index distribution. A grating with low modulation (*seed grating*) would exist within the medium which could be enhanced by SED like by a developing process.

The result of such an experiment is shown in figure 2. The grating is written for only 0.2 s, what is much shorter than the response time of the medium, and then read by the pump wave only. The intensity of the created wave increases within 20 s up to a value many times higher than immediately after the write process. Therefore, one can conclude that the diffraction efficiency and with this the refractive index modulation n_1 is increased. As expected, the decrease of the thickness of the grating leads to a decreasing diffraction efficiency after reaching its maximum and finally to a complete erasure of the hologram.

The erasure of gratings in BCT by white light was investigated. A hologram is written by two waves interfering within the medium. Then, the crystal is homogeneously illuminated by white light. In order to investigate the response of the hologram, it is read out by the former pump wave. The intensity of the wave that is created is measured.

Results are shown in figure 3. Once, the pump wave is switched on only for short time periods, so that the grating is nearly not influ-

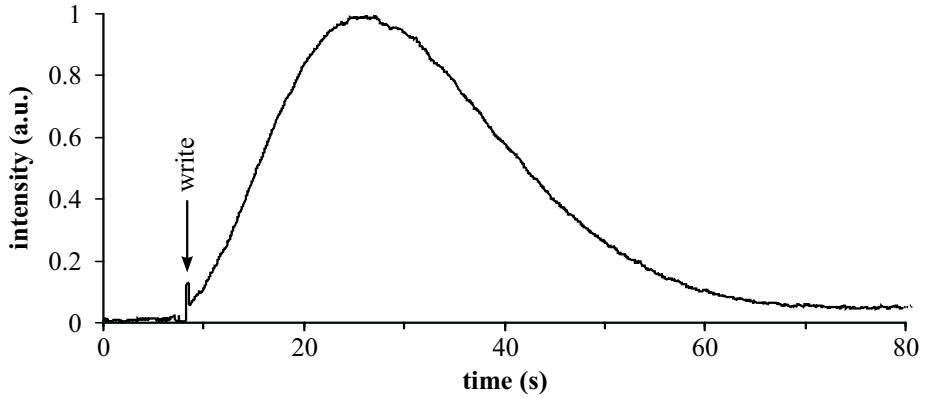

Fig. 2: Build-up of a hologram from a *seed grating* by SED. Temporal behaviour of the intensity of the wave that is created by the readout. The *seed grating* is written for 0.2 s with $I_p = 20\,\mathrm{mW/mm^2}$ and $I_s = 20\,\mathrm{nW/mm^2}$.

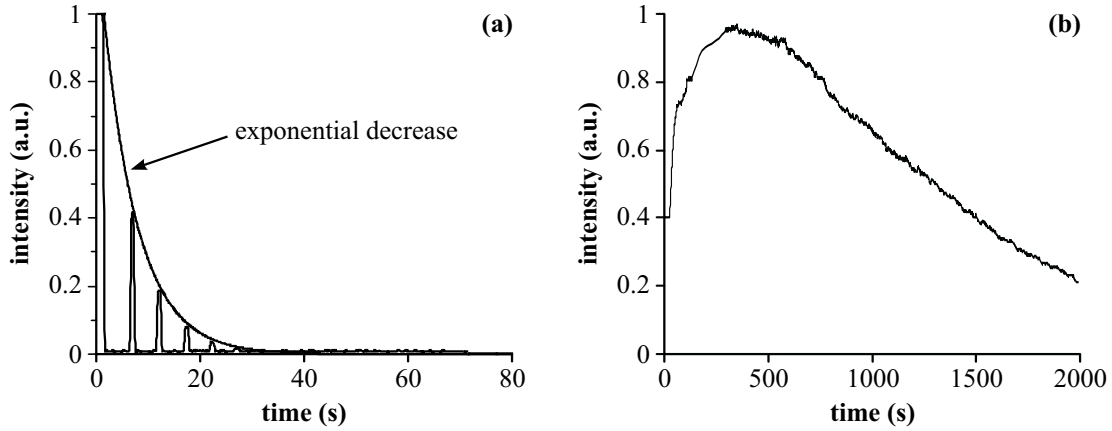

Fig. 3: Temporal course of the intensity of the read out wave during erasure with white light **(a)** without SED and **(b)** with SED. $I_p = I_s = I_{white} = 10\,\mathrm{mW/mm^2}$.

enced by the reading (fig. 3a). The other time, the hologram is read continuously so that the SED can work. In the first case an exponential decrease appears as was to be expected. An exponential function which was fitted to the data was drawn in figure 3a. The time for erasure is in the range of 30 s for this intensities. In the second case the SED leads to a rewriting of the grating and to a higher stability against erasure. The erasure time is therefore in the range of 1 h.

The effect of self-enhanced diffraction can be used in order to extend the storage and read times of a hologram, to enhance its refractive index modulation, and to reach a higher stability against erasure by white light.

References

[1] Campbell S, Yeh P, Gu C, Lin S-H, Cheng Ch-J, Hsu K Y, Opt. Lett. 20, 330 (1995)

[2] Esselbach M, Kiessling A, Kowarschik R, SPIE 3749, 450 (1999)

Multiplexing using self-enhanced diffraction

M. Esselbach, A. Kiessling, G. Cedilnik, and R. Kowarschik

A technique that allows to store many holograms within a medium (in this case a photorefractive crystal) and enables them to be read independently is called *multiplexing*. One of the best known methods is the angle multiplexing. There the holograms are written with different angles between signal wave and the reference waves (fig. 1). The separation during reading

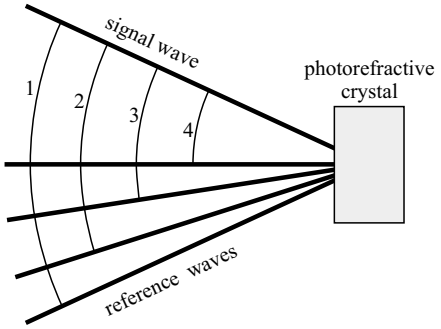

Fig. 1: Angle multiplexing (schematic). $\theta_{1,2,3,4}$ are the different angles between the signal wave and the reference waves.

is possible by the necessity to fulfil the Bragg condition (thick gratings).

It is important to note that, using this method, the diffraction efficiency for each hologram is inversely proportional to the square of the total number of holograms which have to be stored [1–3]. A system for optical information processing always needs a minimum intensity (because of the limited sensitivity of media and sensors) and the intensity of the reading wave (reference wave) can not be increased unlimited (destruction limit). Therefore, the maximal number of holograms is possibly limited by the above mentioned decrease of the diffraction efficiency.

The application of Barium-Calcium-Titanate (BCT) crystals which enables strong interaction of waves that leads to the so-called *self-enhanced diffraction* (SED) and the possibility to write gratings with a low modulation of the intensity distribution could be a solution.

Figure 2 shows the result of an appropriate experiment. Hologram 1 is written with the angle θ_1 between signal and reference wave. After that, a second hologram is written under the angle θ_2. Then, the hologram 1 is read under the angle θ_1. In the first moment the diffraction

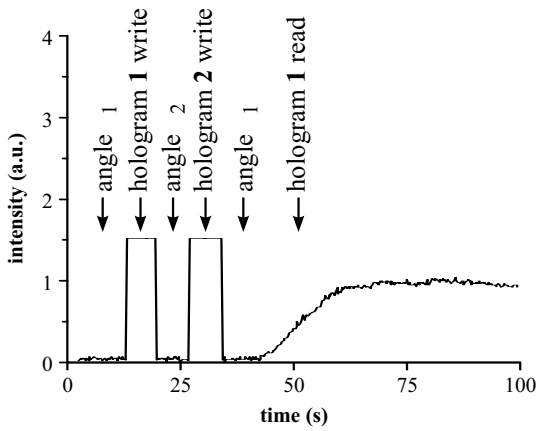

Fig. 2: Angle multiplexing in BCT using SED. Intensity of the wave that is created by reading the appropriate hologram as a function of time. $I_{\text{reference}} = I_{\text{signal}} = 10\,\text{mW/mm}^2$.

efficiency at this hologram is very low, because there is only a weakly modulated *seed grating* [4], and therefore only a low intensity of the reconstructed wave is detectable. But in the following time the modulation of the hologram and with this its diffraction efficiency is increased by the SED [4].

Our experiment is limited to the multiplexing of only two holograms for better clarity. If more holograms are stored and therefore the diffraction efficiency of each hologram decreases, that hologram which is to be read will be amplified (higher refractive index modulation) by the read process itself. The stored information can be handled, that means the reconstructed wave has enough intensity to be practically used.

References

[1] Burr G W, Ashley J, Coufal H, Grygier R K, Hoffnagel J A, Jefferson C M, Marcus B, Opt. Lett. 22, 639 (1997)

[2] Alves C, Pauliat G, Roosen G, *Holographic memories with photorefractive materials*, in F. Agulló-López (Editor), *Insulating materials for optoelectronics: New developments*, World Scientific, Singapore (1995)

[3] Burr G W, Chou W, Neifeld M A, Coufal H, Hoffnagel J A, Jefferson C M, Appl. Opt. 37, 5431 (1998)

[4] Esselbach M, Dissertation, Jena (1999)

Reflections on information storage with optical and other methods

M. Esselbach

One of the main wishes of people which work in the field of information processing is the realisation of an optical computer. This is a device that can manage all the tasks of a computer as information input, processing, output and storage on a purely optical way. The initial euphoria, with which this goal was pursued, a little abated when it became clear that though the realizability of many of the optical components could be shown, the practical realisation of an working system would still require a great deal of expenditure of research. In addition, optical information processing systems have to compete with established and rapidly developing electronic systems. Their theoretical limits of performance are indeed much higher.

Therefore, it seems to be appropriate to develop pure optical components for certain tasks, for which the optics is destined. This would be above all any pre-processing of information for instance with special filters [1,2] and the storage of information [3–5].

Optical storage media as the Compact Disk are common today and the computer technique is unthinkable without them in these times. Nevertheless, its storage capacity still can be increased but it is limited by the two-dimensional storage principle. Extensive studies of possibilities for increasing the storage capacities are documented in the literature, where often methods are used in a modified form that are usually applied for the high resolution analysis of surfaces.

Non-optical techniques for surface manipulation on atomic level using scanning probe microscopy (SPM), atomic force microscopy (AFM) and scanning tunnel microscopy (STM) [6] are worth mentioning. SPM enables removing and depositing of single atoms or a nanometer-scale cluster with field evaporation and micro-scratch deformation, and also to carry a single atom using the Van der Waals force. AFM and STM enable the placement of single atoms (namely gold because of the high chemical resistance) on a surface made from silicon dioxide. Well known are the words IBM and HITACHI [6] written with a number of gold atoms (or small clusters) as a demonstration of the realizability and the capability of the method. A lateral resolution of approximately 80 nm could be reached in their experiments, but the positioning of single atoms could be shown.

Electron beam lithography also enables high-resolution structuring of surfaces. Electron beam poling of polymer layers [7] could be a suited technology together with second harmonic generation (SHG) or FOURIER-transform infrared spectroscopy as methods for an optical reading of the stored information.

Assuming an atom diameter in the range of 1 Å and the presence or absence of an atom at a certain position on the surface as a possibility to store one Bit of information a storage density of 10^{16} Bit/cm^2 would be imaginable theoretically applying *atomic storage*. If we ignore all the technical difficulties, that let these methods seem to be fiction from today's point of view, and assume a 1000 fold parallel writing and reading of the information with a frequency of 1 MHz, more than 100 days would be necessary to write all the 1 cm^2 memory.

This shows a principal handicap of all serial methods for information storage purposes. The speed of writing and retrieval is much to low for amounts of data that are to be handled already today.

An optical technique for structuring a surface with a resolution in the range of some nanometers is given by the near-field microscopy [6]. This method uses the evanescent wave at the end of a waveguide with a diameter smaller than the wavelength. That way, the resolution limitation of usual optical free-space propagation systems is evaded. The writing of information could be optomagnetic using the FARADAY effect to read the information [6], Surface-enhanced RAMAN optical data storage (SERODS, [8]) could be used too. When using these methods one has of course to accept their scanning and therefore serial character with the disadvantage mentioned before.

The main advantage of conventional optical information processing in comparison with usual electronic and the above mentioned systems is the inherent parallelism. That means, the information to be handled exists in form of two-dimensional intensity or phase distributi-

ons (pages, images). For usual optical systems a lateral resolution limitation in the range of the wavelength has to be taken into consideration. This disadvantage can be compensated with using three-dimensional media in combination with holographic storage [3,9]. The holography enables multiplexing techniques. So the amount of information within each image (each unit of information) is limited by the limited resolution, but many holograms can be written within one volume of the storage medium without influencing each other. The advantage of parallelism and of the high speed with which data can be handled is kept, because such stores enable page oriented writing and reading of information with random access.

Optical storage systems can for instance be designed as associative memories to make a preprocessing possible. Photorefractive media as real-time media seem to be especially suited for this purpose, because they enable writing, reading, erasing and therefore updating of information.

Multiplexing techniques enable an enormous increase of the storage density and are therefore an especially important topic in research. Some practical realisations are listed and described in the following.

- BRAGG multiplexing. The separation of the holograms is reached by writing and reading with various wavelengths [10,11] and/or various angles between signal and reference wave [10,12,13] and the necessity to fulfil the BRAGG condition.
- Electric field multiplexing, using the controllable wavelength change within the medium by means of the electrooptic effect and an externally applied electric field with various strengths [14].
- Shift multiplexing, spherical or at least nonplane reference wave and lateral shift of the medium between the recording processes of two holograms [15–18].
- Spatial multiplexing, holograms are recorded in sub-volumes [19].
- Peristrophic multiplexing, rotation of the storage medium around the bisector of the angle between signal and reference wave [20,21].
- Phase-coding, using a bundle of reference waves with defined phase differences to each other (usually $\pi/2$) [22,23]. The code system for accessing pages (certain holograms) is given by the order of reference waves with phase differences of 0 or $\pi/2$ in that way that all other holograms read with the bundle of waves add to zero by interference and only the one that is accessed does not.
- Spectral hole burning, narrow-band controlling of the absorption [24], enables highgrade multiplexing but the experimental expenditure is high too (tuneable lasers, cooling down to $\approx 4\,\mathrm{K}$).
- Fractal multiplexing, angle change of the reference wave each time between write and read processes [19] (BRAGG mismatch).

Some of these methods can be combined, what greatly increases the number of independently recordable holograms per crystal [25].

Three-dimensional holographic storage media are far superior to conventional two-dimensional media (CD, DVD, magnetooptical memory) because of their *volume properties*. This is also true if techniques as the near field optics are included. There is a series of estimations about the reachable storage density in 3D media in the literature [26] that span some orders of magnitude. One of the surely best-founded is $2 \cdot 10^{15}\,\mathrm{Bit/cm^3}$ [19] for binary data and a wavelength of 500 nm. This approximately means the storage of 250 Bits within a cube with edges as long as the wavelength. Using intensity coding (grey values) a further increase by a factor of $2 \ldots 5$ [19] is possible in dependence on the signal-to-noise ratio of the system. One single data page could have a data density up to $10^7\,\mathrm{Bit/cm^2}$.

In conclusion, the holographic optical data storage is still in its infancy but the theoretical possibilities are enormous and the research in this direction is promising [27].

References

[1] M. Esselbach, A. Kiessling, H. Rehn, B. Fleck, R. Kowarschik, J. Opt. Soc. Am. B 14, 846 (1997)

[2] H. Rehn, R. Kowarschik, Appl. Opt. 34, 4907 (1995)

[3] F.T.S. Yu, S. Jutamulia (Ed.), *Optical storage and retrieval*, Marcel Dekker, New York (1996)

[4] M. Esselbach, G. Cedilnik, A. Kiessling, R. Kowarschik, J. Opt. A: Pure Appl. Opt. 1, 21 (1999)

[5] M. Esselbach, G. Cedilnik, A. Kiessling, R. Kowarschik, J. Mod. Opt. 46, 1977 (1999)

[6] R. Imura, H. Koyanagi, M. Miyamoto, T. Shintani, K. Nakamura, A. Kikukawa, S. Hosaka, SPIE 2338, Proc. 1994 Topical meeting on optical data storage, 56 (1994)

[7] R. Danz. A. Büchtemann, M. Pinnow, A. Wedel, SPIE 2338, Proc. 1994 Topical meeting on optical data storage, 352 (1994)

[8] T. Vo-Dinh, SPIE 2338, Proc. 1994 Topical meeting on optical data storage, 148 (1994)

[9] A.D. McAulay, *Optical computer architectures*, John Wiley & Sons, New York (1991)

[10] I. McMichael, W. Christian, D. Pletcher, T.Y. Chang, J.H. Hong, Appl. Opt. 35, 2375 (1996)

[11] T. Kume, K. Nonaka, M. Yamamoto, S. Yagi, Appl. Opt. 37, 334 (1998)

[12] D. Lande, J.F. Heanue, M.C. Bashaw, L. Hesselink, Opt. Lett. 21, 1780 (1996)

[13] F.H. Mok, Opt. Lett. 18, 915 (1993)

[14] M. Balberg, M. Razvag, E. Refaeli, A.J. Agranat, Appl. Opt. 37, 841 (1998)

[15] D. Psaltis, M. Levene, A. Pu, G. Barbastathis, K. Curtis, Opt. Lett. 20, 782 (1995)

[16] G. Barbastathis, D. Psaltis, Opt. Lett. 21, 432 (1996)

[17] S. Tao, D.R. Selviah, J.E. Midwinter, Opt. Lett. 18, 912 (1993)

[18] Y.H. Kang, K.H. Kim, B. Lee, Opt. Lett. 22, 739 (1997)

[19] C. Alves, G. Pauliat, G. Roosen, *Holographic memories with photorefractive materials*, in F. Agulló-López (Editor), *Insulating materials for optoelectronics: New developments*, World Scientific, Singapore (1995)

[20] E. Chuang, D. Psaltis, Appl. Opt. 36, 8445 (1997)

[21] K. Curtis, A. Pu, D. Psaltis, Opt. Lett. 19, 993 (1994)

[22] C. Denz, G. Pauliat, G. Roosen, T. Tschudi, Opt. Comm. 85, 171 (1991)

[23] C. Denz, G. Pauliat, G. Roosen, T. Tschudi, Appl. Opt. 31, 5700 (1992)

[24] E.S. Maniloff, S.B. Altner, S. Bernet, F.R. Graf, A. Renn, U.P. Wild, Appl. Opt. 34, 4140 (1995)

[25] D. Psaltis, D.G. Stinson, G.S. Kino, *Optical data storage: Three perspectives*, T.M. Milster (Editor), OSA Optics & Photonics News, 35 (November 1997)

[26] G.W. Burr, W. Chou, M.A. Neifeld, H. Coufal, J.A. Hoffnagel, C.M. Jefferson, Appl. Opt. 37, 5431 (1998)

[27] M. Esselbach, *Optische Speicherung und Verarbeitung von Information mit photorefraktiven Medien*, Dissertation, Jena (1999)

Non-continuous resonator for dynamic optical storage

M. Esselbach, G. Cedilnik, A. Kiessling

Because of the real-time properties of photorefractive media, which are suited and necessary for the realisation of write-read optical memories, the stored information is erased by reading as well as by updating of information. Possibilities to take remedial measure are to work with extreme low intensities for reading [1], what is no principal solution because it only slows down the erase process, or to use fixing techniques. Extensive descriptions of such methods that of course limit the possibilities for updating and with this principally the use of optical-holographic systems for reversible information storage and processing are given in reference [2].

Another method for keeping the stored information is the utilisation of dynamic or refresh techniques, which are extensively studied in references [3–6]. Using a method called OSIRIS [3], the information stored in a photorefractive crystal is incessantly read out, transmitted into an auxiliary memory and from this back into the crystal again and in this way refreshed. Phase-correct back-coupling by means of nonlinear optical phase conjugation is used. Figure 1 shows the principle. How it works is described

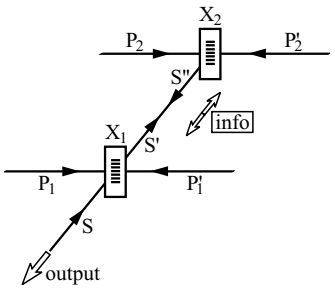

Fig. 1: Memory setup, $X_{1,2}$ are BT crystals.

in references [3–5].

The gratings in crystal X_1 are written first by the waves S and P_1 and after one cycle by P_1' and S''. Both gratings have an identical shape because phase conjugation is used. Because the wave S'' is created by reading crystal X_2 by P_2' there can be a phase shift between original and refreshed grating that depends on the phase difference between the waves P_1' and P_2'. The same applies to the gratings in crystal X_2 where the phase shift between one grating and the grating that is written after passing the next cycle depends on the phase difference between the waves P_1 and P_2. So, there is an unavoidable gradual phase shift always between one grating and the following. This would lead to a superposition of shifted gratings inside each crystal and therefore after a certain number of cycles the gratings will be levelled and the information erased. This is an inherent problem to all such continuously working systems [3,6]. In order to avoid this we introduce a procedure within each cycle (see figure 2) where the grating that has been read (and therefore already has been erased in some degree) is erased completely by white light. That way, each time only

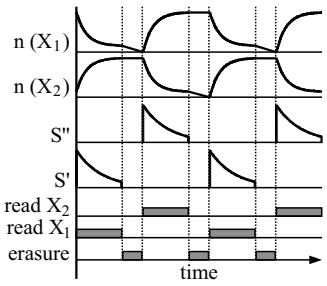

Fig. 2: Course of the refresh cycles. Δn is the amplitude of the refractive index modulation.

one grating exists within one crystal and gradual erasure is avoided [3]. That way a unlimited storage could be reached of course under acceptance of a higher experimental expenditure.

References

[1] J. Colin, S. Bann, H. Rajbenbach, J.-P. Huignard, Appl. Opt. 36, 9304 (1997)

[2] C. Alves, G. Pauliat, G. Roosen, *Holographic memories with photorefractive materials*, in F. Agulló-López (Editor), *Insulating materials for optoelectronics: New developments*, World Scientific, Singapore (1995)

[3] M. Esselbach, G. Cedilnik, A. Kiessling, R. Kowarschik, J. Opt. A: Pure Appl. Opt. 1, 21 (1999)

[4] M. Esselbach, G. Cedilnik, A. Kiessling, R. Kowarschik, J. Mod. Opt. 46, 1977 (1999)

[5] M. Esselbach, G. Cedilnik, A. Kiessling, R. Kowarschik, Optics & Laser Technology, accepted for publication (1999)

[6] T. Dellwig, C. Denz, T. Rauch, T. Tschudi, Opt. Lett. 119, 333 (1995)

New findings about transient fanning in fiberlike Sillenites

M. Esselbach, G. Cedilnik, and A. Kiessling

Fanning, an asymmetrically amplified scattering, appears with fiberlike Sillenite crystals because high gain can be reached applying strong AC fields [1]. The experimental arrangement used for our studies is shown in the left part of figure 1. Fanning builds up after switching on

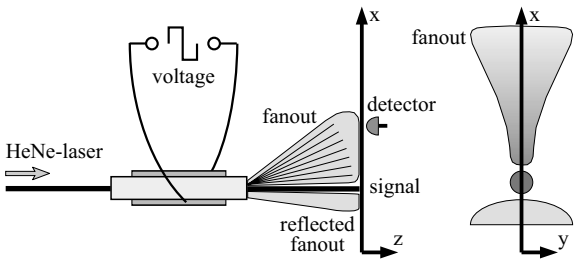

Fig. 1: Experimental arrangement (left) and the intensity distribution observable on a screen (right, schematically).

the externally applied voltage and can be observed on a screen (fig. 1 right side). This process enables the coupling of 90 % of the signal wave power into the fanout.

Because of the so-called *Giant Momentary Readout* [2] this effect is especially strong in the moment when the external AC voltage changes its sign. Then *transient fanning* and a so-called *fanning wave* occur [3]. At first the maximum of the fanout is within a small angle range near the signal wave and then moves along the x-axis to larger angles, according to higher spatial frequencies of the holographic gratings. The result is a spatially and temporally varying intensity structure. Figure 2 shows a series of photographs of the fanout on a screen. Using a point

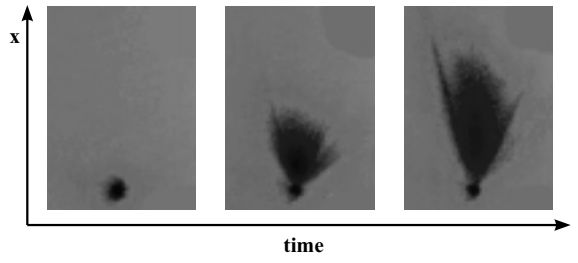

Fig. 2: Photographs of the fanning (contrast inverse).

detector at a certain position on the x-axis far from the crystal (fig. 1) and measuring the intensity in dependence on time one observes a short time increase followed by a maximum (after the time τ_p) and a decrease when the fanning wave passes the detector. Transient fanning is based on the dependence of the response time of the photorefractive effect on the grating period Λ according [4,5]

$$\tau_\mathrm{p} = \frac{\epsilon h c\, \gamma_\mathrm{r} N_\mathrm{A}}{\lambda \upsilon \beta I_0 \mu q} \times \frac{\left(1+\frac{\mu q E_\mathrm{d}}{\gamma_\mathrm{r}\epsilon E_\mathrm{q}}\right)^2 + \left(\frac{\mu q}{\gamma_\mathrm{r}\epsilon E_\mathrm{q}}\right) E_0^2}{\left(1+\frac{\mu q E_\mathrm{d}}{\gamma_\mathrm{r}\epsilon E_\mathrm{q}}\right)\left(1+\frac{E_\mathrm{d}}{E_\mathrm{q}}\right) + \left(\frac{\mu q}{\gamma_\mathrm{r}\epsilon E_\mathrm{q}^2}\right) E_0^2} \quad (1)$$

where h is the PLANCK constant, c the speed of light, μ the mobility of the charge carriers, υ the absorption coefficient, β the quantum efficiency of the photo-excitation, γ_r the recombination rate, N_A the acceptor density, λ the wave length, q the unit charge, E_d the diffusion field, E_q the saturation field, and E_0 the externally applied electric field.

It turns out that the response is faster for larger Λ and therefore smaller angles ϑ between the interacting waves. At first these parts of the fanning, that is initially propagating in all directions, are amplified by the signal wave (only one wave falls onto the crystal) which have small angles to this wave, and only in the following time more and more energy is coupled into larger angle ranges.

Figure 3 shows the the result of a measurement of the dependence of τ_p on the angle ϑ. The curve is calculated according to equation

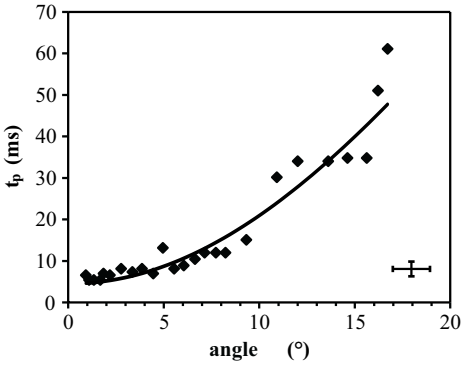

Fig. 3: Dependence of the response time of the fanning on the angle with respect to the signal wave.

(1). N_A and μ/γ_r are used as variable parameters to fit the curve to the measured values, because they are known to vary strongly between

different crystals [5]. The good correspondence is obvious. For more detailed studies the depletion of the signal wave and the energy coupling of the fanout waves between each other had to be considered. Equation (1) was originally derived only for two-wave mixing with undepleted pump wave. Now, fanning is a multi-two-wave mixing process.

Nevertheless, this equation seems to be suited for a description within a large angle range.

References

[1] E. Nippolainen, V.V. Prokofiev, A.A. Kamshilin, T. Jaaskelainen, G. Cedilnik, M. Esselbach, A. Kiessling, R. Kowarschik, OSA TOPS 27, 333 (1999)

[2] E. Shamonina, K.H. Ringhofer, B.I. Sturman, V.P. Kamenov, G. Cedilnik, M. Esselbach, A. Kiessling, R. Kowarschik, A.A. Kamshilin, V.V. Prokofiev, T. Jaaskelainen, Opt. Lett. 23, 1435 (1998)

[3] E. Raita, A.A. Kamshilin, V.V. Prokofiev, T. Jaaskelainen, Appl. Phys. Lett. 70, 1641 (1997)

[4] S.I. Stepanov, M.P. Petrov, Opt. Comm. 53, 292 (1985)

[5] A.A. Kamshilin, E. Raita, V.V. Prokofiev, T. Jaaskelainen, Appl. Phys. Lett. 67, 3242 (1995)

Temporal behaviour of SPPCM described with two-wave mixing

M. Esselbach and A. Kiessling

The build-up behaviour of self-pumped phase conjugate mirrors (PCM) has been studied in the literature with great interest. The references [1–3] are especially worth mentioning. There the conditions are investigated that enable the build-up of the pc-reflection based on noise (fanning). Some simplified models [3–5] describe the pc-process in SPPCM with the assumption of two four-wave mixing centres within the photorefractive crystal. The exact description of the build-up is difficult, because this is a self-organising process [6,7], through which its dynamic is difficult to understand [1] and can even show chaotic behaviour [8]. Models that are closer to reality often use numerical methods [9–11].

Figure 1 shows the temporal development of the reflectivity of a so-called cat-PCM and an ESPPCM (realised in barium titanate) that are experimentally observed. The response of the

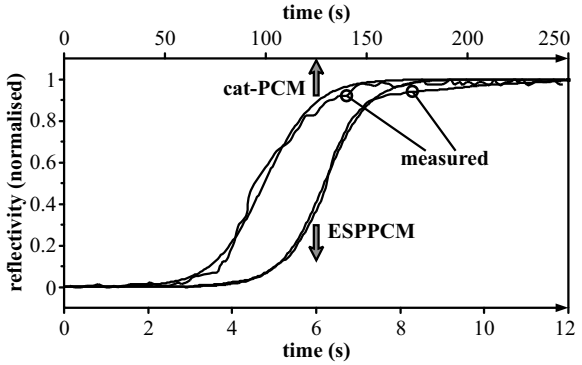

Fig. 1: Build-up of the pc-reflection of cat-PCM and ESPPCM ($\lambda = 514\,\mathrm{nm}$, $I = 10\,\mathrm{mW/mm^2}$).

ESPPCM is much faster than of the cat-PCM (note the two scales in the figure), what was found already earlier [12].

In order to find a formal description one can proceed from a time dependent coupling constant Γ of the TWM in the form

$$\Gamma(t) = \Gamma_\infty \left(1 - \mathrm{e}^{-\frac{t}{\tau}}\right) \qquad (1)$$

where τ is a response time and Γ_∞ is the value of Γ for the steady state. In the first moment of the build-up the phase conjugated wave is created by FWM, then this wave is amplified by the reading pump wave via simple TWM. With $\Gamma(t)$ and using the coupled wave equations it is possible to yield the expression

$$R(t) = R_\infty \left(\frac{1}{1 + \mathrm{e}^{-\frac{(t-\tau_\mathrm{s})}{\tau_\mathrm{pc}}}} - \frac{1}{1 + \mathrm{e}^{\frac{\tau_\mathrm{s}}{\tau_\mathrm{pc}}}} \right) \qquad (2)$$

for the temporal behaviour of the reflectivity R, where τ_pc is the response time of the phase conjugation process and τ_s is given by the length of the so-called *silent zone* [1].

Figure 1 shows functions according to equation (2) that are fitted by varying Γ_∞, τ_s, and τ_pc. The good correspondence of measured and calculated behaviour is obvious.

In conclusion, the pc-process in SPPCM can be described by a time dependent TWM, but the necessary parameters can not be simply deduced from the material properties until now.

References

[1] N.I. Bel'dyugina, A.V. Mamaev, V.V. Shkunov, Appl. Opt. 32, 3962 (1993)

[2] I.C. Khoo, N.I. Bel'dyugina, H. Li, A.V. Mamaev, V.V. Shkunov, Opt. Lett. 18, 473 (1993)

[3] A.A. Zozulya, IEEE J. Quantum Electron. 29, 538 (1993)

[4] P. Yeh, Wiley Series in Pure and Applied Optics, John Wiley & Sons, New York (1993)

[5] L. Solymar, D.J. Webb, A. Grunnet-Jepson, Oxford series in optical and imaging sciences, Clarendon Press, Oxford (1994)

[6] R. Kowarschik, L. Wenke, T. Baade, M. Esselbach, A. Kiessling, G. Notni, K. Uhlendorf, Appl. Phys. B, im Druck (1999)

[7] Y. Zheng, A. Sasaki, X. Gao, H. Aoyama, Opt. Lett. 20, 267 (1995)

[8] P.M. Jeffrey, R.W. Eason, J. Opt. Soc. Am. B 11, 476 (1994)

[9] Z. Zhang, Y. Lian, S.X. Dou, P. Ye, Opt. Comm. 110, 631 (1994)

[10] Z. Zhang, Y. Zhang, C. Yang, J. Kang, S. Zheng, Y. Zhu, Y. Chen, X. Wu, P. Fu, J. Opt. Soc. Am. B 11, 1992 (1994)

[11] A.A. Zozulya, M. Saffman, D.Z. Anderson, Phys. Rev. Lett. 73, 818 (1994)

[12] H. Rehn, R. Kowarschik, Opt. Comm. 109, 155 (1994)

Erasure of holographic gratings in BCT by white light

M. Esselbach, G. Cedilnik, and A. Kiessling

The effect of white light for erasure of refractive index gratings in photorefractive crystals is studied. This is especially of interest if such crystals shall be used as media for holographic information storage [1–3]. If the optical memory should offer a possibility to update the stored information, the former gratings have to be erased. In optical systems for dynamic information storage the erasure of gratings within each cycle is a part of the storage process itself [1]. Barium-Calcium-Titanate seems to be an interesting and promising medium for the realisation of optical memories and therefore is should be studied concerning its behaviour with during light erasure.

A hologram is written by illuminating the crystal with the interference pattern of signal and pump wave. We have chosen an intensity ratio of $m_\mathrm{v} = 1$. Then the crystal is homogeneously illuminated by white light. In order to observe the strength of the grating that is kept within the crystal in spite of erasing for a certain time the hologram is read by the pump wave and the intensity of the diffracted wave is measured.

Results are shown in figures 1 and 2. In figure 1 the hologram is read periodically for a short time by switching on the pump wave. Therefore

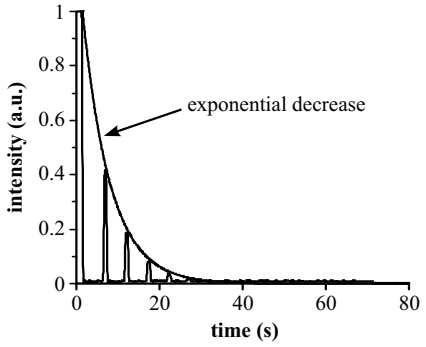

Fig. 1: Intensity of the read wave as a function of time with erasure by white light with pump wave **off** (only switched on for the short time period of the measurement). $I_\mathrm{p} = I_\mathrm{s} = I_\mathrm{white} = 10\,\mathrm{mW/mm^2}$.

the grating is nearly not influenced by the read process. In figure 2 the grating is continuously read. The signal wave was switched of all the time during the measurements.

In the first case we observed a behaviour as expected, an exponential decrease. An exponential function has been fitted to the measured curve and shows a good correspondence (see fig. 1). We assume a dependence of the erasure response time τ on the intensity I_white of the white light nearly in the form $\tau \sim 1/I_\mathrm{white}$, but this should not be verified within these studies. With the given intensities the erasure time is in the range of 10 s.

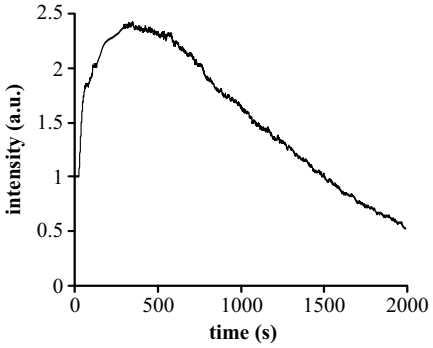

Fig. 2: Intensity of the read wave as a function of time with erasure by white light with pump wave **on**. $I_\mathrm{p} = I_\mathrm{s} = I_\mathrm{white} = 10\,\mathrm{mW/mm^2}$.

In the second case we observe an absolutely different behaviour. The intensity of the diffracted wave at first increases and then decreases, but with a much slower response. The approximated response time is 0.5 h. We suggest to assume that this behaviour is based on the self-enhanced diffraction which yields a re-writing and even an amplification of the grating during the reading [4].

The result is a higher stability against white light what can mean an advantage or a disadvantage depending on the intention.

References

[1] M. Esselbach, G. Cedilnik, A. Kiessling, R. Kowarschik, J. Opt. A: Pure Appl. Opt. 1, 21 (1999)

[2] M. Esselbach, G. Cedilnik, A. Kiessling, R. Kowarschik, J. Mod. Opt. 46, 1977 (1999)

[3] M. Esselbach, G. Cedilnik, A. Kiessling, R. Kowarschik, Optics & Laser Tech., in press (1999)

[4] M. Esselbach, Dissertation, Jena (1999)